

# Covariant calculation of nonstrange decays of strange baryon resonances

T. Melde, W. Plessas, B. Sengl

*Theoretische Physik, Institut für Physik, Karl-Franzens-Universität, Universitätsplatz 5, A-8010 Graz, Austria*

We report on a study of  $\pi$  and  $\eta$  decays of strange baryon resonances within relativistic constituent-quark models based on one-gluon-exchange and Goldstone-boson-exchange dynamics. The investigations are performed in the point form of Poincaré-invariant relativistic quantum mechanics with a spectator-model decay operator. The covariant predictions of the constituent-quark models underestimate the experimental data in most cases. These findings are congruent with an earlier study of nonstrange baryon decays in the light-flavor sector. We also consider a nonrelativistic reduction of the point-form spectator model, which leads to the decay operator of the elementary emission model. For some decays the nonrelativistic results differ substantially from the relativistic ones and they exhibit no uniform behavior as they scatter above and below the experimental decay widths.

PACS numbers: 12.39.Ki, 13.30.Eg, 14.20.Jn

Keywords: Relativistic constituent quark model; hadronic baryon decays; hyperons

## I. INTRODUCTION

Strong decay processes still present a considerable challenge within the physics of hadrons. This is unfortunate, not only in view of the vast amount of experimental data but also because the decay properties of hadron resonances give important insights into strong interaction physics (see, for example, the recent NSTAR workshops [1, 2, 3]). Investigations of strong decay processes date back to the late 1960s [4, 5, 6, 7, 8], and with the refinement of constituent quark models (CQMs) various aspects of the strong decays have been studied [9, 10, 11, 12, 13, 14, 15, 16, 17, 18, 19, 20]. In particular, the decay mechanism and the type of hyperfine interactions in CQMs have been in the focus of interest. These investigations have been performed within nonrelativistic or so-called relativised models, and usually a number of parameters has been introduced beyond the CQMs employed. Further complications resulted in the ambiguity of the proper phase space factor and various forms have been used. As a consequence the available results are strongly dependent on the chosen inputs. This makes them hardly comparable to each other, and from the comparison with experiment the quality of the CQMs cannot be judged reliably.

In our investigations we are primarily interested in the direct predictions of decay widths by different types of CQMs. Once they are established on a consistent basis for all decay modes, one can go ahead to study particular details of the decay mechanism as well as baryon wave functions. Recently, we presented a covariant calculation of  $\pi$  and  $\eta$  decays of  $N$  and  $\Delta$  resonances with relativistic CQMs of the one-gluon-exchange (OGE) and Goldstone-boson-exchange (GBE) types [21]. The investigations were performed in the framework of Poincaré-invariant quantum mechanics [22]. In particular, we adhered to its point-form version [23, 24, 25] and applied a spectator-model decay operator. In this way the transition amplitude could be calculated in a manifestly covariant manner and ambiguities regarding the phase-space factor could be avoided.

Here we report on the extension of our study of  $\pi$  and  $\eta$  decays to strange baryon resonances. Again we work with the relativistic GBE and OGE CQMs of Refs. [26, 27] and [20], respectively.

While there is a wealth of experimental data on these types of decays, theoretical investigations are rather scarce in the literature, at least within modern CQMs; in particular, we are not aware of any relativistic calculations. There exists an older study of strange resonance decays [5] but the corresponding results are mainly of a qualitative nature. More recently, since the advent of CQMs, there have only been a few investigations of strong decays in the strange sector [9, 18, 19, 28].

In Section II we briefly describe the theoretical framework of the relativistic calculations with the PFSM decay operator; the nonrelativistic limit is delegated to the Appendix A. In Sections IV and V we present the numerical results for decay widths in the  $\pi$ - and  $\eta$ -channels, respectively. Finally, in Section VI, we summarize our findings and give a conclusion.

## II. THEORY

The decay width of a hadron resonance is defined by the expression

$$\Gamma_{i \rightarrow f} = \frac{|\vec{q}|}{4M^2} \frac{1}{2J+1} \times \sum_{M_J, M_{J'}} \frac{1}{2T+1} \sum_{M_T, M_{T'}, M_{T_m}} |F_{i \rightarrow f}|^2, \quad (1)$$

with the transition amplitude  $F_{i \rightarrow f}$  given by the matrix element of the four-momentum conserving reduced decay operator  $\hat{D}_{rd}^m$  between incoming and outgoing hadron states

$$F_{i \rightarrow f} = \langle V', M', J', M_{J'}, T', M_{T'} | \hat{D}_{rd}^m | V, M, J, M_J, T, M_T \rangle, \quad (2)$$

where  $m$  refers to the particular mesonic decay mode. In our case,  $q_\mu = (q_0, \vec{q})$  denotes the four-momentum of the outgoing meson in the rest-frame of the decaying baryon resonance. The latter is expressed by the eigenstate  $|V, M, J, M_J, T, M_T\rangle$ , characterized by the eigenvalues of the velocity  $V$ , mass  $M$ , intrinsic spin  $J$  with z-component  $M_J$ , and isospin  $T$  with z-projection  $M_T$ ; correspondingly the outgoing baryon state is denoted by

primed eigenvalues. The baryon eigenstates are obtained by the solution of the eigenvalue problem of the invariant mass operator  $\hat{M}$  including the interactions. They are simultaneously eigenstates of the baryon four-velocity  $\hat{V}^\mu$ .

Representing the baryon eigenstates with suitable basis states the matrix element in Eq. (2) can be evaluated by the following integral

$$\begin{aligned} \langle V', M', J', M_{J'}, T', M_{T'} | \hat{D}_{rd}^m | V, M, J, M_J, T, M_T \rangle &= \frac{2}{MM'} \sum_{\sigma_i \sigma'_i} \sum_{\mu_i \mu'_i} \int d^3 \vec{k}_2 d^3 \vec{k}_3 d^3 \vec{k}'_2 d^3 \vec{k}'_3 \\ &\times \sqrt{\frac{(\sum_i \omega'_i)^3}{\prod_i 2\omega'_i}} \Psi_{M' J' M_{J'} T' M_{T'}}^* \left( \vec{k}'_1, \vec{k}'_2, \vec{k}'_3; \mu'_1, \mu'_2, \mu'_3 \right) \prod_{\sigma'_i} D_{\sigma'_i \mu'_i}^{*\frac{1}{2}} \{R_W[k'_i; B(V')]\} \\ &\times \langle p'_1, p'_2, p'_3; \sigma'_1, \sigma'_2, \sigma'_3 | \hat{D}_{rd}^m | p_1, p_2, p_3; \sigma_1, \sigma_2, \sigma_3 \rangle \\ &\times \prod_{\sigma_i} D_{\sigma_i \mu_i}^{\frac{1}{2}} \{R_W[k_i; B(V)]\} \sqrt{\frac{(\sum_i \omega_i)^3}{\prod_i 2\omega_i}} \Psi_{M J M_J T M_T} \left( \vec{k}_1, \vec{k}_2, \vec{k}_3; \mu_1, \mu_2, \mu_3 \right). \end{aligned} \quad (3)$$

Herein,  $\Psi_{M J M_J T M_T}(\vec{k}_1, \vec{k}_2, \vec{k}_3; \mu_1, \mu_2, \mu_3)$  represents the rest-frame wave function of the incoming baryon, where the  $\mu_i$  refer to the spin projections of the three quarks  $i = 1, 2, 3$ , and their three-momenta  $\vec{k}_i$  sum up to zero; analogously,  $\Psi_{M' J' M_{J'} T' M_{T'}}^*(\vec{k}'_1, \vec{k}'_2, \vec{k}'_3; \mu'_1, \mu'_2, \mu'_3)$  is the rest-frame wave function of the outgoing baryon. These wave functions result from the velocity-state representations of the baryon eigenstates (for more details of the formalism see Ref. [21]). The Wigner rotations stem from the boosts of the baryon eigenstates relating the individual quark momenta through  $p_i = B(V)k_i$ . The momentum representation of the decay operator follows from the PFSM construction, which assumes that only one of the quarks directly couples to the emitted meson, while the other two act as spectators:

$$\begin{aligned} &\langle p'_1, p'_2, p'_3; \sigma'_1, \sigma'_2, \sigma'_3 | \hat{D}_{rd}^m | p_1, p_2, p_3; \sigma_1, \sigma_2, \sigma_3 \rangle \\ &= -3\mathcal{N} \frac{ig_{qqm}}{2m_1} \frac{1}{\sqrt{2\pi}} \bar{u}(p'_1, \sigma'_1) \gamma_5 \gamma^\mu \mathcal{F}^m u(p_1, \sigma_1) q_\mu \\ &2p_{20} \delta^3(\vec{p}_2 - \vec{p}'_2) \delta_{\sigma_2 \sigma'_2} 2p_{30} \delta^3(\vec{p}_3 - \vec{p}'_3) \delta_{\sigma_3 \sigma'_3}. \end{aligned} \quad (4)$$

Here,  $g_{qqm}$  is the quark-meson coupling constant,  $m_1$  the mass of the active quark,  $\mathcal{F}^m$  the flavor-transition operator specifying the particular decay mode, and  $u(p_1, \sigma_1)$  the quark spinor according to the standard notation [29]; details of the formalism can be found in Ref. [30].

The factor  $\mathcal{N}$  is specific for the PFSM construction [31] and is taken to be

$$\mathcal{N} = \left( \frac{M}{\sum_i \omega_i} \frac{M'}{\sum_i \omega'_i} \right)^{\frac{3}{2}}. \quad (5)$$

This form is congruent with the calculations in Ref. [21] and also consistent with the requirements of baryon charge normalisation as well as time-reversal invariance of the electromagnetic form-factors [32]. The same normalisation factor was also used in previous studies of the electroweak structure of the nucleons and the other light and strange baryon ground states [33, 34, 35, 36].

We also consider a nonrelativistic reduction of the PFSM decay operator. Its derivation is given in the Appendix A and it leads to the standard impulse approximation according to the elementary emission model (EEM):

$$\begin{aligned} &\langle p'_1, p'_2, p'_3; \mu'_1, \mu'_2, \mu'_3 | \hat{D}_{rd}^{m, NR} | p_1, p_2, p_3; \mu_1, \mu_2, \mu_3 \rangle \\ &\propto \frac{\mathcal{F}^m}{2m_1} \left\{ \vec{\sigma}_1 \cdot \vec{q} - \frac{\omega_m}{2m_1} \vec{\sigma}_1 \cdot (\vec{p}_1 + \vec{p}'_1) \right\} \\ &\times 2p_{20} \delta^3(\vec{p}_2 - \vec{p}'_2) \delta_{\mu_2 \mu'_2} 2p_{30} \delta^3(\vec{p}_3 - \vec{p}'_3) \delta_{\mu_3 \mu'_3}. \end{aligned} \quad (6)$$

### III. CONSTITUENT-QUARK MODELS

For the calculations of the mesonic decay widths we employ two different kinds of relativistic CQMs. Thereby we can learn about the importance of distinct hyperfine interactions. In particular, we consider the GBE CQM [26] and the OGE CQM in the variant of the relativistic version of the Bhaduri-Cohler-Nogami model [38] as parameterised by Theussl et al. [20]. The invariant mass spectra of both CQMs are shown in Fig. 1 in comparison to experiment as compiled by the Particle Data Group (PDG) [37].

The spectra of the two CQMs show the typical be-

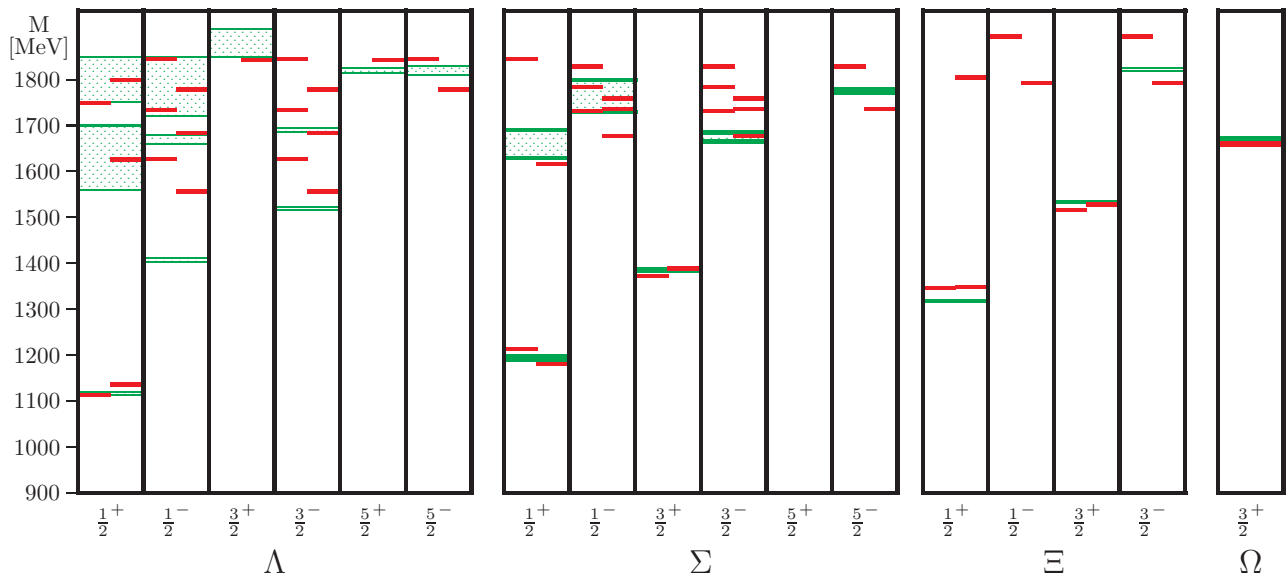


FIG. 1: Energy levels (solid lines) of the lowest  $\Lambda$ ,  $\Sigma$ ,  $\Xi$ , and  $\Omega$  states with intrinsic spin and parity  $J^P$  for the OGE (left levels) and GBE (right levels) CQMs as presented in Refs. [20] and [26], respectively. The shadowed boxes represent the experimental values with their uncertainties [37].

havior as it is well known from the literature [27]. Only the flavor-dependent hyperfine interaction of the GBE CQM is able to reproduce at the same time the correct level orderings in the nucleon and the  $\Lambda$  excitation spectra [26]. Both types of CQMs fail in reproducing the  $\Lambda(1405)$  resonance. Further shortcomings of the CQMs may also reside in other strange baryon excitations, for which no experimental data exist at the moment. Differences between theoretical and experimental resonance masses, however, can have a strong influence on the predictions for decay widths. In order to have these mass effects under control, we calculated the decay widths by using also experimental masses as input. In this way we can directly estimate the effects from different quark-model wave functions too.

#### IV. DIRECT PREDICTIONS OF $\pi$ DECAY WIDTHS

In Table I we present the direct predictions of the  $\pi$  decay widths for strange baryon resonances. The relativistic results have been obtained with the PFSM decay operator with pseudovector coupling as specified in Eq. (4). The nonrelativistic results correspond to the calculation with the EEM transition operator as given in Eq. (6). For both cases theoretical masses (as predicted by the particular CQMs) and experimental masses (as quoted by the PDG [37]) have been employed.

In general the present results for the  $\pi$  decay widths of the strange baryon resonances parallel the ones obtained earlier in case of the nonstrange resonances [21]: the covariant predictions usually underestimate the experimental data or at most reach them from below. Here, there

are only a few notable exceptions, namely the decays of  $\Lambda(1405)$  and  $\Lambda(1670)$  going to  $\Sigma\pi$ . In the first case the overshooting of the experimental value is only present, if the theoretical resonance masses are used. It disappears when employing the experimental resonance mass. Therefore we may attribute the large values for the decay widths essentially to the theoretical overpredictions of the  $\Lambda(1405)$  mass, both by the GBE and OGE CQMs. The situation is not so clear-cut with regard to the  $\Lambda(1670)$ . Its resonance mass is more or less reproduced in accordance with the experimental data, at least in case of the GBE CQM; still the decay widths are predicted far too high. There is only a minor mass effect in these overpredictions, since they are also not reduced when employing the experimental resonance mass. Therefore we may suspect the large  $\pi$  decay widths of  $\Lambda(1670)$  to be caused by another reason, possibly a coupling of resonance states.

Of particular interest is the decay of the  $\Sigma(1750)$   $\frac{1}{2}^-$  resonance to  $\Sigma\pi$ . From the spectrum as presented in Fig. 1 we observe three theoretical levels for each CQM, and it appears natural to identify the lowest lying  $J^P = \frac{1}{2}^-$  state with the  $\Sigma(1750)$  resonance, which is the only  $\frac{1}{2}^-$   $\Sigma$  excitation with at least three-star status in the PDG compilation. The predictions for the  $\pi$  decay widths of this lowest lying state turn out to be much bigger than the experimental value measured for the  $\Sigma(1750)$ ; the corresponding figures can be found under the entry of  $\Sigma(1750)^1$  in Table I. However, we may also consider the two other theoretical levels in the  $J^P = \frac{1}{2}^-$  excitation spectrum as candidates for  $\Sigma(1750)$ . Upon calculating their  $\pi$  decay widths we find the predictions as given under the entries of  $\Sigma(1750)^2$  and  $\Sigma(1750)^3$  in Table I. Surprisingly, the theoretical results for the

TABLE I: Covariant predictions for  $\pi$  decay widths by the GBE CQM [26] and the OGE CQM [20] in comparison to experiment. The first three columns classify the decaying resonance according to the PDG [37]. The relativistic calculations have been performed along the PFSM, and the EEM results represent their nonrelativistic limits. We used both theoretical and experimental masses (best estimates of the PDG) as input. For comparison we present in the last column also the results of a nonrelativistic calculation by Koniuk and Isgur [9].

Decay	$J^P$	Experiment [MeV]	Theoretical Mass				Experimental Mass				Literature
			Relativistic		Nonrel. EEM		Relativistic		Nonrel. EEM		
			GBE	OGE	GBE	OGE	GBE	OGE	GBE	OGE	
$\rightarrow \Sigma\pi$											
$\Lambda(1405)$	$\frac{1}{2}^-$	$(50 \pm 2)$	55	78	320	611	15	17	76	112	55
$\Lambda(1520)$	$\frac{3}{2}^-$	$(6.55 \pm 0.16)^{+0.04}_{-0.04}$	5	9	5	8	2.8	3.1	2.1	2.3	7.8
$\Lambda(1600)$	$\frac{1}{2}^+$	$(53 \pm 38)^{+60}_{-10}$	3	33	2	34	3	17	1.2	15	14
$\Lambda(1670)$	$\frac{1}{2}^-$	$(14.0 \pm 5.3)^{+8.3}_{-2.5}$	69	103	620	1272	68	94	572	1071	10
$\Lambda(1690)$	$\frac{3}{2}^-$	$(18 \pm 6)^{+4}_{-2}$	19	25	24	28	18	21	23	22	44
$\Lambda(1800)$	$\frac{1}{2}^-$	<i>seen</i>	68	101	473	1175	70	95	485	1095	121
$\Lambda(1810)$	$\frac{1}{2}^+$	$(38 \pm 23)^{+40}_{-10}$	3.8	2.1	55	150	4.1	5.0	55	94	36
$\Lambda(1830)$	$\frac{5}{2}^-$	$(52 \pm 19)^{+11}_{-12}$	14	19	16	24	16	20	22	24	59
$\Sigma(1385)$	$\frac{3}{2}^+$	$(4.2 \pm 0.5)^{+0.7}_{-0.5}$	3.1	0.5	6.5	1.1	2.0	2.1	4.1	4.8	7.8
$\Sigma(1660)$	$\frac{1}{2}^+$	<i>seen</i>	10	24	2	15	12	14	2.4	6.9	14
$\Sigma(1670)$	$\frac{3}{2}^-$	$(27 \pm 9)^{+12}_{-6}$	15	23	21	32	13	17	17	21	44
$\Sigma(1750)^1$	$\frac{1}{2}^-$	$(3.6 \pm 3.6)^{+5.6}_{-0}$	58	102	480	1249	63	102	574	1402	
$\Sigma(1750)^2$	$\frac{1}{2}^-$	$(3.6 \pm 3.6)^{+5.6}_{-0}$	32	44	135	312	32	38	136	262	
$\Sigma(1750)^3$	$\frac{1}{2}^-$	$(3.6 \pm 3.6)^{+5.6}_{-0}$	10	1.0	116	34	10	0.9	110	32	0.25
$\Sigma(1775)$	$\frac{5}{2}^-$	$(4.2 \pm 1.8)^{+0.8}_{-0.3}$	1.9	3.8	2.9	6.9	2.2	3.2	3.5	5.3	6
$\Sigma(1940)$	$\frac{3}{2}^-$	<i>seen</i>	2.2	3.7	0.5	1.1	4.9	5.8	1.6	2.4	19
$\rightarrow \Lambda\pi$											
$\Sigma(1385)$	$\frac{3}{2}^+$	$(31.3 \pm 0.5)^{+4.4}_{-4.3}$	11	11	25	28	14	13	31	32	44
$\Sigma(1660)$	$\frac{1}{2}^+$	<i>seen</i>	8	5	6	0.02	10	3	8	0.05	8.4
$\Sigma(1670)$	$\frac{3}{2}^-$	$(6 \pm 3)^{+3}_{-1}$	2.5	2.0	5.5	5.1	2.7	1.5	6.0	3.2	5.8
$\Sigma(1750)^1$	$\frac{1}{2}^-$	<i>seen</i>	1.6	1.5	43	67	0.8	1.4	49	70	
$\Sigma(1750)^2$	$\frac{1}{2}^-$	<i>seen</i>	19	25	160	422	18	25	169	359	
$\Sigma(1750)^3$	$\frac{1}{2}^-$	<i>seen</i>	1.0	2.8	18	105	0.9	3	18	97	28
$\Sigma(1775)$	$\frac{5}{2}^-$	$(20 \pm 4)^{+3}_{-2}$	6	10	10	21	8	8	15	15	22
$\Sigma(1940)$	$\frac{3}{2}^-$	<i>seen</i>	0.2	0.4	1.7	3.5	0.5	0.5	5.9	6.1	0.16
$\rightarrow \Xi\pi$											
$\Xi(1530)$	$\frac{3}{2}^+$	$(9.9)^{+1.7}_{-1.9}$	2.2	1.3	4.4	3.0	5.5	5.3	11.4	12.5	
$\Xi(1820)$	$\frac{3}{2}^-$	<i>seen</i>	0.4	1.6	0.3	1.4	0.7	1.2	0.6	0.9	

last one are pretty consistent with the magnitude of the experimental value for  $\Sigma(1750)$ . It is thus suggested to identify the third level  $\Sigma(1750)^3$  with the experimentally measured  $\Sigma(1750)$ . The two remaining eigenstates are then left to be interpreted as the lower lying resonances  $\Sigma(1620)$  and maybe  $\Sigma(1560)$ , which are observed in experiment with only two-star status [40].

The influences from different hyperfine interactions in the CQMs can be estimated by comparing the results obtained with the experimental masses in the eighth and ninth columns of Table I. In general, they are small. Considerable differences are seen only for the  $\Lambda(1600)$  and  $\Sigma(1750)^3$  in the  $\Sigma\pi$  channel as well as for  $\Sigma(1660)$  and  $\Sigma(1750)^3$  in the  $\Lambda\pi$  channel.

Let us finally have a look at the results from the non-relativistic reduction of the PFSM, leading to the EEM. One can hardly find a common trend among the non-relativistic EEM predictions. Rather they scatter below and above the experimental data. Evidently, the non-relativistic approximation causes huge enhancements of the decay widths for the  $J^P = \frac{1}{2}^-$  resonances. They become way too high as compared to experiment. On the other hand, the  $J^P = \frac{1}{2}^+$  decay widths are much reduced by the nonrelativistic approximation, with the exception of the  $\Lambda(1810)$ . For the  $J^P = \frac{3}{2}^-$  resonances the nonrelativistic results are very similar to the relativistic ones, with the exception of the  $\Sigma(1940)$ . As we have kept the phase-space factor fixed, this behavior of the nonrelativistic approximation is governed only by the truncation in the spin couplings and the elimination of Lorentz boosts. This makes the effects of the nonrelativistic reduction strongly dependent on the decaying resonance. As a result any nonrelativistic approximation for calculating decay widths must be taken with considerable doubt.

In the last column of Table I we also quote the predictions of Koniuk and Isgur (KI) [9] and we observe a completely different behaviour than in any of our calculations. Especially, the KI results are seen in rather good agreement with experimental data (except for the case of  $\Lambda(1690)$ , whose decay width comes out too large). It has to be noted, however, that KI introduced additional parameters to fit their quark model predictions to experiment in order to generally investigate the feasibility of decay calculations within constituent quark models. We, on the other hand, refrained from applying any parameterisation beyond the direct PFSM predictions quoted in Table I, as we are interested in the pure nature of the relativistic results and their dependences on the dynamics of different CQMs. Once this step is clarified, we can proceed to refine the decay calculations in order to possibly arrive at a more convincing description of hadronic decays [41].

## V. DIRECT PREDICTIONS OF $\eta$ DECAY WIDTHS

As a second nonstrange decay mode of strange baryon resonances we consider the  $\eta$  decays of  $\Lambda$  and  $\Sigma$ , the results of which are given in Table II. Regarding the predictions of the GBE CQM in case of theoretical masses we observe that the  $\eta$  decays of the  $\frac{1}{2}^-$   $\Lambda(1670)$  and  $\frac{3}{2}^-$   $\Lambda(1690)$  resonances (which are degenerate in our calculation) are not possible energetically, since the mass eigenvalue of 1136 MeV for the  $\Lambda$  ground state lies slightly too high. On the other hand, the  $\Lambda(1670)$  decay width of the OGE CQM obviously results too big, in accordance with the fact that the  $\Lambda(1670)$  mass lies too high. These deficiencies become repaired when the experimental masses are employed. The  $\eta$  decay widths of the  $\Lambda(1670)$  then

come out reasonably for both the GBE and OGE CQMs, and they are found in agreement with the experimental data as well as the KI results. The  $\eta$  decay width of the  $\Lambda(1690)$  is in all instances extremely small.

The biggest  $\eta$  decay width is predicted for the  $\frac{1}{2}^-$   $\Lambda(1800)$  resonance by both the GBE and OGE CQMs; also the corresponding KI result is the largest one among all  $\eta$  decays. Already the  $\pi$  decay width of this state has been found to be rather large in all cases above (cf., Table I). The PDG does not present any data for non-strange partial decay widths. Given the fact that the total decay width of  $\Lambda(1800)$  is of the order of 200–400 MeV [37], the interpretation of the large  $\pi$  and  $\eta$  decays should not pose any particular problem, however.

The remaining  $\eta$  decays of the  $\Lambda(1810)$  and  $\Lambda(1830)$  are predicted to be rather small by both the GBE and OGE CQMs. Similar results are reported also from the KI calculation.

Regarding the  $\eta$  decays of the  $\Sigma(1750)$  resonance we again quote the widths of all three states that can a priori be considered as candidates for this resonance. The relatively largest decay width is obtained by the GBE CQM for the  $\Sigma(1750)^3$  state. It almost reaches the experimental data band from below. In the previous section this state was interpreted as the proper candidate for the  $\Sigma(1750)$  resonance, whereas the  $\Sigma(1750)^1$  and the  $\Sigma(1750)^2$  states should rather be identified with the  $\Sigma(1560)$  and  $\Sigma(1620)$  resonances, respectively. We now find this interpretation further substantiated by the  $\eta$  decays.

In summary we note that the only  $\eta$  decays with appreciable decay widths are the ones of  $\Lambda(1670)$ ,  $\Lambda(1800)$ ,  $\Lambda(1830)$ , and  $\Sigma(1750)$ . It is interesting to note that the octet partners of the former two in the light-flavor sector, namely, the  $N(1535)$  and  $N(1650)$  resonances, are just the ones with appreciable sizes for  $N \rightarrow N\eta$  decay widths.

The nonrelativistic reduction again has a considerable effect on the  $\eta$  decay widths. As observed in case of the  $\Pi$  decays, it enhances in particular the results for the  $\frac{1}{2}^-$  states. The corresponding figures appear way too big at least for the  $\Lambda(1670)$  and  $\Lambda(1800)$  resonances. On the other hand, the decay widths of the  $\frac{3}{2}^-$  are again reduced and practically vanish.

## VI. CONCLUSIONS

We have reported relativistic calculations of non-strange decays of strange baryon resonances within CQMs. In particular, we have presented covariant predictions for  $\pi$  and  $\eta$  decays of  $\Lambda$ ,  $\Sigma$ , and  $\Xi$  resonances by two types of CQMs, the ones with GBE and OGE dynamics. The transition elements have been calculated with a spectator-model decay operator in point-form relativistic quantum mechanics. The present results complement the ones obtained earlier for the same mesonic decay modes

TABLE II: Same as Table I, but for the  $\eta$ -decay channels.

Decay	$J^P$	Experiment [MeV]	Theoretical Mass				Experimental Mass				Literature
			Relativistic		Nonrel. EEM		Relativistic		Nonrel. EEM		
			GBE	OGE	GBE	OGE	GBE	OGE	GBE	OGE	
$\rightarrow \Lambda\eta$											
$\Lambda(1670)$	$\frac{1}{2}^-$	$(6.1 \pm 2.6)^{+3.8}_{-2.5}$	—	19	—	151	4	6	22	44	4.8
$\Lambda(1690)$	$\frac{3}{2}^-$		—	0.2	—	0.08	0.02	0.02	$\approx 0$	$\approx 0$	0.01
$\Lambda(1800)$	$\frac{1}{2}^-$		43	65	223	624	46	62	264	526	15
$\Lambda(1810)$	$\frac{1}{2}^+$		0.9	$\approx 0$	2.8	6.3	0.7	0.7	3.9	2.3	1.7
$\Lambda(1830)$	$\frac{5}{2}^-$		0.6	2.2	0.4	1.6	2.0	1.8	1.6	1.3	5.3
$\rightarrow \Sigma\eta$											
$\Sigma(1750)^1$	$\frac{1}{2}^-$	$(31.5 \pm 18.0)^{+38.5}_{-4.5}$	—	—	—	—	5	11	25	71	3
$\Sigma(1750)^2$	$\frac{1}{2}^-$	$(31.5 \pm 18.0)^{+38.5}_{-4.5}$	3.0	3.1	1.5	5.0	0.6	3.8	4.7	1.9	
$\Sigma(1750)^3$	$\frac{1}{2}^-$	$(31.5 \pm 18.0)^{+38.5}_{-4.5}$	6.0	2.1	25	10	3.8	1.4	14	6.3	
$\Sigma(1775)$	$\frac{5}{2}^-$		$\approx 0$	0.05	$\approx 0$	$\approx 0$	0.02	0.01	$\approx 0$	$\approx 0$	
$\Sigma(1940)$	$\frac{3}{2}^-$		$\approx 0$	$\approx 0$	$\approx 0$	$\approx 0$	$\approx 0$	0.02	0.07	0.01	

of the (nonstrange)  $N$  and  $\Delta$  resonances [21].

Regarding the  $\pi$  decay widths we have found that the direct relativistic predictions of the CQMs in general underestimate the experimental data. In this respect the results parallel the ones obtained earlier for  $N$  and  $\Delta$  resonances along the same approach. Here, only the  $\Lambda(1670)$  represents an exception. We argue that a possible mixing effect with the  $\Lambda(1405)$  resonance is responsible for this result. Such mixings of resonance states should certainly be taken into account in a future more refined calculation.

The systematics of the relativistic results has also led to a new interpretation of the three lowest  $\frac{1}{2}^- \Sigma$  excitations produced by the CQMs. In principle, all three can be seen as candidates for the phenomenological  $\Sigma(1750)$ . However, most naturally only the third state  $\Sigma(1750)^3$  is identified with the experimentally measured  $\Sigma(1750)$ , as it produces the most adequate  $\pi$  decay width.

For the  $\eta$  decay widths we have found a qualitatively similar behavior, namely, they are all rather small or at most reach the (scarce) experimental data from below. Even the largest  $\eta$  decay width of  $\Lambda(1800)$  can be characterized in this manner, since its total decay width is reported to be extremely large.

In the present work we have also shown that the PFSM decay operator has a sensible nonrelativistic reduction, leading to the standard elementary-emission model. However, it has also become evident that the nonrelativistic decay widths exhibit no consistent pattern, as they vary considerably in their magnitudes, scattering above and below the experimental data. The nonrelativistic reduction introduces sizable effects strongly depending on the  $J^P$  values of the pertinent resonances.

We have herewith completed the relativistic studies of

$\pi$  and  $\eta$  decays of light and strange baryon resonances within CQMs. We have established the direct predictions of two types of CQMs without introducing any additional parameterisations. The results show a consistent behavior but they are not able to explain the experimental data. In any case relativistic effects are found to be of utmost importance. The present study provides for a reliable starting point to improve the relativistic description of mesonic decays.

### Acknowledgments

This work was supported by the Austrian Science Fund (FWF-Projects P16945 and P19035). B. S. acknowledges support by the Doctoral Program 'Hadrons in Vacuum, Nuclei and Stars' (FWF-Project W1203). The authors have profited from valuable discussions with L. Canton, A. Krassnigg, and R.F. Wagenbrunn.

### APPENDIX A: DETAILS OF THE NONRELATIVISTIC REDUCTION

In the following we specify the nonrelativistic reduction of the PFSM calculation that leads to the EEM. We leave the invariant phase-space factor in Eq. (1) untouched and start with the matrix element of the reduced decay operator in Eq. (2)

$$\begin{aligned}
 F_{i \rightarrow f} = & \langle V', M', J', M_{J'}, T', M_{T'} | \hat{D}_{rd}^m | V, M, J, M_J, T, M_T \rangle = \\
 & \langle P', J', M_{J'}, T', M_{T'} | \hat{D}_{rd}^m | P, J, M_J, T, M_T \rangle, \quad (\text{A1})
 \end{aligned}$$

which is now expressed in terms of momentum eigenstates  $|P, J, M_J, T, M_T\rangle$ . In a first step we replace in this matrix element the Lorentz boosts by Galilean boosts and use free three-quark states  $|\vec{k}_2, \vec{k}_3, \vec{P}; \mu_1, \mu_2, \mu_3\rangle$  instead of velocity states for the representation of the eigenstates of the quark-model Hamiltonian. This leads to baryon wave functions in the form

$$\begin{aligned} & \langle \vec{k}'_2, \vec{k}'_3, \vec{P}'; \mu'_1, \mu'_2, \mu'_3 | \vec{P}, J, M_J, T, M_T \rangle \\ &= \Psi_{MJM_JTM_T} \left( \vec{k}'_1, \vec{k}'_2, \vec{k}'_3; \mu'_1, \mu'_2, \mu'_3 \right) \delta^3 \left( \vec{P}' - \vec{P} \right), \end{aligned} \quad (\text{A2})$$

where the completeness relation of the free three-quark states reads

$$\mathbf{1} = \sum_{\mu_1, \mu_2, \mu_3} \int d^3k_2 d^3k_3 d^3P \times |\vec{k}_2, \vec{k}_3, \vec{P}; \mu_1, \mu_2, \mu_3\rangle \langle \vec{k}_2, \vec{k}_3, \vec{P}; \mu_1, \mu_2, \mu_3|. \quad (\text{A3})$$

Using the latter one obtains for the spectator-model decay operator of Eq. (4) the following expression

$$\begin{aligned} F_{i \rightarrow f}^{NR} &= \langle P', J', M_{J'}, T', M_{T'} | \hat{D}_{rd}^{m, NR} | P, J, M_J, T, M_T \rangle \\ &= \sqrt{2E} \sqrt{2E'} \sum_{\mu_i \mu'_i} \int d^3k_2 d^3k_3 \Psi_{M'J'M_{J'}T'M_{T'}}^* \left( \vec{k}'_1, \vec{k}'_2, \vec{k}'_3; \mu'_1, \mu'_2, \mu'_3 \right) \\ &\times \frac{-3\mathcal{N}}{\sqrt{2p_{10}}\sqrt{2p'_{10}}} \frac{g_{qqm}}{2m_1} \frac{1}{\sqrt{2\pi}} \bar{u}(p'_1, \mu'_1) \gamma_5 \gamma^\mu \mathcal{F}^m u(p_1, \mu_1) q_\mu \delta_{\mu_2\mu'_2} \delta_{\mu_3\mu'_3} \Psi_{MJM_JTM_T} \left( \vec{k}_1, \vec{k}_2, \vec{k}_3; \mu_1, \mu_2, \mu_3 \right), \end{aligned} \quad (\text{A4})$$

where  $E, E'$  are the energies of the decaying and final baryons. Similarly,  $p_{10}$  and  $p'_{10}$  denote the energies of the active quark in the incoming and outgoing channels, respectively. The nonrelativistic baryon momenta satisfy  $\vec{P} = \sum \vec{p}_i$  as well as  $\vec{P}' = \sum \vec{p}'_i$ . In addition, the energy and the momentum of the emitted meson are given by  $\omega_m = E - E' = p_{10} - p'_{10}$  and  $\vec{q} = \vec{P} - \vec{P}' = \vec{p}_1 - \vec{p}'_1$ , respectively.

Next we have to express the various variables in Eq. (A4) in terms of the residual integration variables  $\vec{k}_2$  and  $\vec{k}_3$ . The corresponding relations are obtained from a nonrelativistic limit of the original Lorentz boosts. This calculation is conveniently carried out in the rest frame of the decaying baryon resonance and leads to the following result

$$\begin{aligned} \vec{p}_1 &= -\vec{k}_2 - \vec{k}_3, \\ \vec{p}'_1 &= -\vec{k}_2 - \vec{k}_3 - \vec{q}, \\ \vec{p}_2 &= \vec{p}'_2 = \vec{k}_2, \\ \vec{p}_3 &= \vec{p}'_3 = \vec{k}_3, \\ \vec{k}'_1 &= -\vec{k}_2 - \vec{k}_3 - \frac{m_2 + m_3}{m_1 + m_2 + m_3} \vec{q}, \\ \vec{k}'_2 &= \vec{k}_2 + \frac{m_2}{m_1 + m_2 + m_3} \vec{q}, \\ \vec{k}'_3 &= \vec{k}_3 + \frac{m_3}{m_1 + m_2 + m_3} \vec{q}. \end{aligned} \quad (\text{A5})$$

Here, one has made the approximations  $M \approx \sum m_i$  as well as  $M' \approx \sum m'_i$ , i.e. the interacting masses of the baryons become equal to the free masses in the nonrelativistic limit; for the decay modes considered in this paper one has furthermore  $m_i = m'_i$ . Furthermore, one neglected terms of the orders  $(\frac{p_q}{m_q})^2$  and  $(\frac{\omega_m}{m_q})^2$ , upon the assumption that the quark masses  $m_i$  are large as compared to the absolute value of the three-momentum  $\vec{p}_i$  and the meson energy  $\omega_m$ .

For the practical calculation one transforms to a coordinate system, where the momentum transfer to the final baryon is into the negative z-direction and obtains for the relations of the primed and unprimed variables  $(\vec{k}'_2, \vec{k}'_3)$  and  $(\vec{k}_2, \vec{k}_3)$

$$\begin{aligned} k'_{ix} &= k_{ix} \\ k'_{iy} &= k_{iy} \\ k'_{iz} &= k_{iz} + \frac{m_i}{m'_1 + m_2 + m_3} Q \end{aligned} \quad (\text{A6})$$

for  $i = 2, 3$ . Here,  $Q$  is the absolute value of the momentum transfer  $\vec{q} = (0, 0, Q)$ . As a consequence of the reduction we also find  $\omega_i \approx m_i$  and  $\omega'_i \approx m'_i$ , which reduces the normalisation factor  $\mathcal{N}$  to 1. The final nonrelativistic reduction for the transition amplitude then reads

$$\begin{aligned}
F_{i \rightarrow f}^{NR} = & \sqrt{2E} \sqrt{2E'} \sum_{\mu_i \mu'_i} \int d^3 \vec{k}_2 d^3 \vec{k}_3 \Psi_{M' J' M_{J'} T' M_{T'}}^* \left( \vec{k}'_1, \vec{k}'_2, \vec{k}'_3; \mu'_1, \mu'_2, \mu'_3 \right) \\
& \times \frac{-3g_{qqm}}{2m_1} \frac{1}{\sqrt{2\pi}} \mathcal{F}^m \left\{ \vec{\sigma}_1 \cdot \vec{q} - \frac{\omega_m}{2m_1} \vec{\sigma}_1 \cdot (\vec{p}_1 + \vec{p}'_1) \right\} \delta_{\mu_2 \mu'_2} \delta_{\mu_3 \mu'_3} \Psi_{M J M_J T M_T} \left( \vec{k}_1, \vec{k}_2, \vec{k}_3; \mu_1, \mu_2, \mu_3 \right). \quad (A7)
\end{aligned}$$

This result represents the familiar expression for the transition amplitude in the EEM, where the terms proportional to  $\vec{\sigma}_1 \cdot \vec{q}$  and  $\vec{\sigma}_1 \cdot (\vec{p}_1 + \vec{p}'_1)$ , involving the Pauli spin operator  $\vec{\sigma}_1$  of the active quark, are called direct and recoil terms, respectively (see, e.g., Refs. [11, 39]). The lat-

ter is specific for the pseudovector coupling in the decay operator (4); it would not be present at the same order of nonrelativistic approximation in case of pseudoscalar coupling.

- 
- [1] in *NSTAR2001, Proceedings of the Workshop on the Physics of Excited Nucleons, Mainz, Germany 7 - 10 March 2001*, edited by D. Drechsel and L. Tiator (World Scientific, Singapore, 2001).
- [2] in *Physics of excited nucleons. Proceedings, Workshop, NSTAR 2002, Pittsburgh, USA, October 9-12, 2002*, edited by S. A. Dytman and E. S. Swanson (World Scientific, Singapore, 2003).
- [3] in *Proceedings of the Workshop on the Physics of Excited Nucleons, Grenoble, France, 24-27 March 2004*, edited by J. P. Bocquet, V. Kuznetsov, and D. Rebreyend (World Scientific, Singapore, 2004).
- [4] C. Becchi and G. Morpurgo, Phys. Rev. **149**, 1284 (1966).
- [5] A. N. Mitra and M. Ross, Phys. Rev. **158**, 1630 (1967).
- [6] D. Faiman and A. W. Hendry, Phys. Rev. **173**, 1720 (1968).
- [7] D. Faiman and A. W. Hendry, Phys. Rev. **180**, 1609 (1969).
- [8] R. P. Feynman, M. Kislinger, and F. Ravndal, Phys. Rev. D **3**, 2706 (1971).
- [9] R. Koniuk and N. Isgur, Phys. Rev. D **21**, 1868 (1980).
- [10] S. Kumano and V. R. Pandharipande, Phys. Rev. D **38**, 146 (1988).
- [11] A. LeYaouanc, L. Oliver, O. Pene, and J. Raynal, *Hadron Transitions in the Quark Model* (Gordon and Breach, New York, 1988).
- [12] F. Stancu and P. Stassart, Phys. Rev. D **38**, 233 (1988).
- [13] F. Stancu and P. Stassart, Phys. Rev. D **39**, 343 (1989).
- [14] S. Capstick and W. Roberts, Phys. Rev. D **47**, 1994 (1993).
- [15] S. Capstick and W. Roberts, Phys. Rev. D **49**, 4570 (1994).
- [16] P. Geiger and E. S. Swanson, Phys. Rev. D **50**, 6855 (1994).
- [17] E. S. Ackleh, T. Barnes, and E. S. Swanson, Phys. Rev. D **54**, 6811 (1996).
- [18] A. Krassnigg *et al.*, Few Body Syst. Suppl. **10**, 391 (1999).
- [19] W. Plessas *et al.*, Few Body Syst. Suppl. **11**, 29 (1999).
- [20] L. Theussl, R. F. Wagenbrunn, B. Desplanques, and W. Plessas, Eur. Phys. J. A **12**, 91 (2001).
- [21] T. Melde, W. Plessas, and R. F. Wagenbrunn, Phys. Rev. C **72**, 015207 (2005); Erratum, Phys. Rev. C **74**, 069901(E) (2006).
- [22] B. D. Keister and W. N. Polyzou, Adv. Nucl. Phys. **20**, 225 (1991).
- [23] P. Dirac, Rev. Mod. Phys. **21**, 392 (1949).
- [24] H. Leutwyler and J. Stern, Ann. Phys. **112**, 94 (1978).
- [25] W. H. Klink, Phys. Rev. C **58**, 3587 (1998).
- [26] L. Y. Glozman, W. Plessas, K. Varga, and R. F. Wagenbrunn, Phys. Rev. D **58**, 094030 (1998).
- [27] L. Y. Glozman, Z. Papp, W. Plessas, K. Varga, and R. F. Wagenbrunn, Phys. Rev. C **57**, 3406 (1998).
- [28] S. Capstick and W. Roberts, Phys. Rev. D **58**, 074011 (1998).
- [29] F. J. Yndurain, *Relativistic Quantum Mechanics and Introduction to Field Theory* (Springer Verlag, Berlin, 1996).
- [30] B. Sengl, Ph.D. thesis, University of Graz, Graz, Austria, 2006.
- [31] T. Melde, L. Canton, W. Plessas, and R. F. Wagenbrunn, Eur. Phys. J. A **25**, 97 (2005).
- [32] T. Melde, L. Canton, W. Plessas, and R. F. Wagenbrunn, nucl-th/0612013 (2006).
- [33] R. F. Wagenbrunn *et al.*, Phys. Lett. **B511**, 33 (2001).
- [34] L. Y. Glozman *et al.*, Phys. Lett. **B516**, 183 (2001).
- [35] S. Boffi *et al.*, Eur. Phys. J. A **14**, 17 (2002).
- [36] K. Berger, R. F. Wagenbrunn, and W. Plessas, Phys. Rev. D **70**, 094027 (2004).
- [37] W.-M. Yao *et al.*, Journal of Physics G **33**, 1+ (2006).
- [38] R. K. Bhaduri, L. E. Cohler, and Y. Nogami, Nuovo Cim. A **65**, 376 (1981).
- [39] T. Ericson and W. Weise, *Pions in Nuclei* (Clarendon Press, Oxford, 1988).
- [40] We note that the eigenstates  $\Sigma(1750)^2$  and  $\Sigma(1750)^3$  can be distinguished by their internal spin structure. It turns out that their ordering is reversed in the OGE CQM, namely the  $\Sigma(1750)^3$  falls below the  $\Sigma(1750)^2$ .
- [41] E.g., one could simply start with varying the quark-meson coupling constant in the decay operator of Eq. (4); so far we adhered to an  $SU(3)$  symmetric choice just as it is employed in the GBE CQM [26, 27]. Of course, one should consider also more substantial improvements of the decay mechanism and in addition of the description of resonance states.